Linear Rheological Properties of the Semifluorinated Copolymer Tetrafluoroethylene-Hexafluoropropylene-Vinylidenfluoride (THV) with Controlled Amounts of Long-Chain Branching

Jens Stange,[†] Susanne Wächter,[‡] and Helmut Münstedt*

University Erlangen-Nürnberg, Institute of Polymer Materials, Department of Materials Science, Martensstrasse 7, D-91058 Erlangen, Germany

Harald Kaspar

Dyneon GmbH & Co. KG, Research Department, Werk Gendorf, D-84504 Burgkirchen, Germany

Received November 22, 2006; Revised Manuscript Received January 12, 2007

ABSTRACT: Various semifluorinated polymers of narrow molar mass distributions and definitely changed molecular structure are employed as model substances to investigate the impact of the polymer architecture on key rheological properties in the linear range of shear flow. These model samples originate from free radical terpolymerizations of tetrafluoroethylene (TFE), hexafluoropropylene (HFP), and vinylidenfluoride (VDF), referred to as THV. They were tailored to cover a broad range of mass-average molar masses of a straight linear and of a long-chain branched topography. By the controlled incorporation of long-chain branches (LCB) into the fluoropolymers, a complex thermorheological behavior is observed. The effect of long-chain branching also becomes evident by dynamic-mechanical measurements represented by a plot of the angle δ versus the complex modulus $|G^*(\omega)|$. Compared to the linear reference materials for which $\eta_0 \sim M_w^{3.8}$ was found, the zero-shear rate viscosity η_0 of some of the branched polymers is significantly higher than that of a linear product with equivalent M_w, for others it comes to lie below the curve for linear samples. The experimental η_0 (M_w) data of the branched THV are in good agreement with an approach proposed by Janzen and Colby using the structural information from the molecular characterization. Moreover, it was found that plotting η_0 as a function of the intrinsic viscosity $[\eta]$ more sensitively discriminates between the various long-chain branched samples than η_0 (M_w). Comparing the sensitivity of methods based on rheological properties in solution and in the molten state, it is demonstrated that the linear behavior of the melts can very favorably be used to get an insight into the molecular architecture of THV polymers.

Introduction

Thermoplastic fluoropolymers such as fluorinated ethylene propylene (FEP), perfluorinated alcoxylene (PFA), or polyvinylidene fluoride (PVDF) become more and more interesting in the field of engineering polymers as they possess a spectrum of excellent properties. The polydispersity factor M_w/M_n of these fluoropolymers typically ranges from 1.6 to 2.7, i.e., they are narrowly distributed in comparison to many other thermoplasts.[1−4]

The consequence of this molecular structure is a lack in processability, particularly in extrusion, due to a low degree of shear thinning. Moreover, the linear fluoropolymers give rise to difficulties in processing operations in which elongational properties dominate due to a weakly pronounced strain hardening. In this aspect, the fluoropolymers are similar to metallocene linear low-density polyethylenes. From this group of polymers, it is well-known that the processing behavior can remarkably be changed by introducing long-chain branching.[5−8]

With some few exceptions, e.g., Maccone et al.,[9] most fluoropolymers produced by conventional methods show a linear chain topography. Therefore, practicable polymerization techniques are on demand, which make it possible to synthesize long-chain branched fluoropolymers. A novel technical route to create THV-polymers with distinct LCB topographies recently became available.[10] Special modifiers are employed in the emulsion polymerization, which induce a certain amount of transfer reactions to the polymer backbone and allow chains to be formed that have a branched structure. The molecular characterization of such THV fluoropolymers was reported recently.[11] These tailor-made fluoropolymers are soluble in some organic solvents, such as tetrahydrofurane, acetone, or methylethylketone, and thus can be investigated in dilute solution with respect to their molecular structure. As it is well-known the analytical methods based on the dissolved molecules have their limitations with respect to the characterization of long-chain branching. Measurements in the molten state are more sensitive in many cases and provide a deeper insight into the molecular architecture. That is the reason why in this paper linear rheological properties of various linear and long-chain branched samples are presented. Making use of the knowledge recently accumulated for polyolefins it is tried to analyze the LCB-THV polymers with respect to the relationship between polymerization conditions and molecular structure.

The influence of branching on the nonlinear rheological behavior of the samples, which allows an assessment of the effect of LCB on processing properties, is discussed elsewhere.[8]

Materials and Experimental

Samples. For this study, tailor-made semifluorinated terpolymers consisting of 39 mol % TFE, 11 mol % HFP, and 50 mol % VDF were used. These model polymers, in the following referred to as THV, were synthesized by means of aqueous emulsion polymerization in a 48.5 L pilot plant reactor (Dyneon GmbH & Co. KG). A set of linear THV terpolymers with varied molar masses was

* Corresponding author. E-mail: polymer@ww.uni-erlangen.de.
[†] Now at Bayer MaterialScience AG, Krefeld, Germany.
[‡] Now at Paul Hartmann AG, Heidenheim/Brenz, Germany.

10.1021/ma0626867 CCC: $37.00
Published on Web 03/03/2007

made. The linear THV samples THV 1 to THV 7 are already described in a former paper by Auhl et al. (2006). For this work, three additional linear THV were synthesized in order to close the gap in the molar mass range between 300 and 700 kg/mol (THV 8 and 9) and to extend the molar mass range up to 10 000 kg/mol (THV 10).

Furthermore, a set of long-chain branched polymers of the same chemical composition was prepared. The amount of LCB and the mass-average molar mass were independently tailored by the amounts of modifier and chain transfer agent employed during the course of polymerization. The set of LCB-THV 1−4 was synthesized with a constant level of chain transfer agent, but with an increasing amount of modifier. As a result, the highest possible number of long-chain branches increased from LCB-THV 1 to LCB-THV 4. The same amount of modifier as for THV 3 was utilized for the preparation of LCB-THV 5 and 6. But due to the different amounts of chain transfer agent employed, different molar masses were obtained.

Molecular Characterization. The characterization of the fluoropolymers with respect to molar mass distribution and degree of long-chain branching was carried out by size-exclusion chromatography (SEC) coupled with a multiangle laser light scattering (MALLS) detector and a refractive index (RI) detector. This method allows a determination of the absolute mass-average molar mass and the radius of gyration of each SEC fraction. The SEC experiments were carried out at 25 °C with analytical grade tetrahydrofuran. A more detailed description of the analytical equipment used is given by Auhl et al.[11] For the three additional linear samples, THV 8−10, the mass-average molar mass was determined by means of solution viscometry using $[\eta] = 5.065 \times 10^{-3} \times M_w^{0.736}$, with $[\eta]$ measured in [mL/g] and M_w in [g/mol].

The intrinsic viscosities $[\eta]$ were obtained from the Huggins equation

$$\eta_{red} = \frac{\eta_{sp}}{c} = [\eta] + k_H \times [\eta]^2 \times c \quad (1)$$

with $k_H = 0.34$, which was independently determined in a former study. The reduced viscosities η_{red} were measured in methylethylketone (MEK) at 35 °C and a concentration c of 2 g/L using a Cannon−Fenske viscometer (Schott AG). The Hagenbach−Couette correction was applied.

Rheological Characterization. Shear rheological measurements were performed using rotational rheometers with a plate−plate geometry of 25 mm in diameter under nitrogen atmosphere. Cylindrical samples of a thickness of 2 mm and a diameter of 23 mm were prepared from press sintered plates. The sintering was performed in a hot press at a temperature of 170 °C. The samples were heated up to 170 °C within 500 s, held under a pressure of 55 bar for 300 s, and cooled down within 200 s. An ARES instrument (Advanced Rheometric Expansion System, Rheometric Scientific) was used for the dynamic-mechanical experiments. Various frequency sweeps were conducted at different temperatures and strain amplitudes typically ranging from 1 to 20%, which is within the linear range of deformation, were applied. Furthermore, steady shear start-up tests at a shear rate of 0.01 s^{-1} were performed. Shear creep measurements were conducted with a constant stress rheometer (CS-Melt, Bohlin). The applied constant shear stresses τ_0 were on the order of 20 Pa, i.e., in the linear range of deformation. Creep times up to $t = 20\,000$ s were needed in order to reach the steady state in the creep tests and to ensure that the steady-state elastic part J_e of the creep compliance $J(t)$ became very small compared to t/η_0. In this case, the zero-shear viscosity can be determined according to:

$$\lim_{\substack{t\to\infty \\ \sigma_0\to 0}} \frac{t}{J(t)} = \eta_0 \quad (2)$$

Results and Discussion

Molecular Characterization. The results of the molecular characterization were already reported in a former paper by Auhl et al.[11] and are summarized shortly in the following. The linear THV samples have a narrow molar mass distribution with polydispersity indices M_w/M_n of well below 2 (see Table 1). They cover a broad range of mass-average molar masses from 160 up to 10 000 kg/mol. The branched character of the long-chain branched THV terpolymers investigated was clearly shown by SEC-MALLS analysis.[11] A distinct tailing at high molar masses for the long-chain branched samples is reflected by a higher polydispersity ($M_w/M_n \approx 3$; see Table 2) compared to the linear references ($M_w/M_n \approx 1.6$). Table 2 also reports the contraction factors g_η measured by solution viscometry and the highest possible number of trifunctional branches per 10^4 C LCB_{max} estimated from the polymerization recipe, as given by Auhl et al.[11] The contraction factors g_η are found to be smaller than 1 for all LCB-THV and, in particular, they decrease with growing numbers of LCB_{max}. This behavior can be explained by an increasing degree of long-chain branching originating from a higher number of branch points incorporated during the course of polymerization. The numbers of trifunctional branches per 10^4 C become higher with the amount of branching modifier added, increasing from LCB-THV 1 to LCB-THV 4. LCB-THV 3, 5, and 6, which were synthesized with the same amount of branching modifier, have a comparable LCB_{max} and thus also

Table 1. Molecular Parameters Determined by SEC-MALLS and Results of the Rheological Characterization of the Linear THV

	M_w [kg/mol]	M_w/M_n[a]	$[\eta]$[b] [mL/g]	η_0 (265 °C) [Pas]
THV 1	161[a]	1.6	33	23
THV 2	242[a]	1.5	46	124
THV 3	725[a]	1.6	105	11 000
THV 4	1450[a]	1.7	171	125 000
THV 5	1870[a]	1.8	214	450 000
THV 6	2480[a]	1.6	309	3 200 000
THV 7	6110[a]	1.8	432	14 500 000
THV 8	309[b]		55	340
THV 9	493[b]		78	2700
THV 10	10 600[b]		665	190 000 000

[a] Determined by SEC coupled with a light-scattering device. [b] Determined in MEK at 35 °C using a Cannon−Fenske viscometer.

Table 2. Molecular Parameters Determined by SEC-MALLS and Results of the Rheological Characterization of the Long-Chain Branched THV Samples

Sample	LCB-THV 1	LCB-THV 2	LCB-THV 3	LCB-THV 4	LCB-THV 5	LCB-THV 6
Modifier	Increasing →				Same as for THV 3	
Chain-transfer agent	Constant				Increasing →	
M_w [kg/mol] [a]	545	684	765	1 030	540	1 316
M_w/M_n [a]	2.4	2.8	2.9	3.2	3.1	2.9
[η] [c] [ml/g]	78	74.5	74.5	84	56	102
$LCB_{max}/10^4C$ [b]	0.3	0.9	2.6	5.3	2.7	2.7
λ [kg/mol] [d]	485	485	630	1 008	315	1 450
M_b [kg/mol] [e]	168	179	223	338	122	468
g_η [c]	0.96	0.77	0.71	0.64	0.65	0.69
η_0 (265 °C) [Pas]	2 780 [f]	5 700 [f]	14 400 [g]	189 000 [g]	1 040 [f]	1 600 000 [g]
η_0 (265 °C) [Pas][h]	2 527	7 016	14 907	-	1 093	-

[a] Determined by SEC coupled with a light-scattering device. [b] Calculated from the amount of branching agent added. [c] $g_\eta = ([\eta]_{LCB}/[\eta]_{lin})_{M_w}$ determined in MEK at 35 °C using a Cannon−Fenske viscometer. [d] Average molar mass of a trifunctional monomeric subunit, determined from the light-scattering data according to the theory of Zimm and Stockmayer.[28] [e] Determined by eqs 8−10. [f] Determined from dynamic-mechanical experiments. [g] Determined from dynamic-mechanical experiments and extrapolation. [h] Determined from creep experiments.

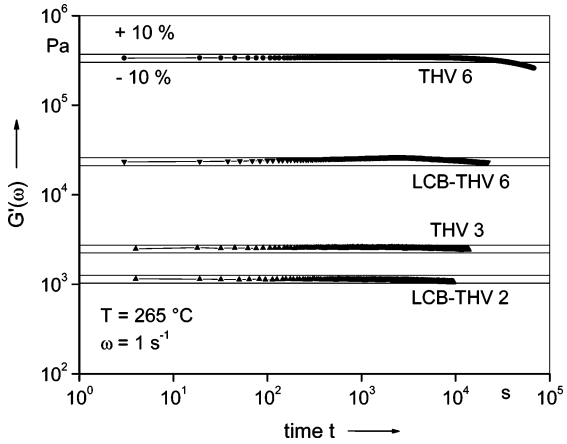

Figure 1. $G'(\omega)$ as a function of time for two linear and two long-chain branched samples.

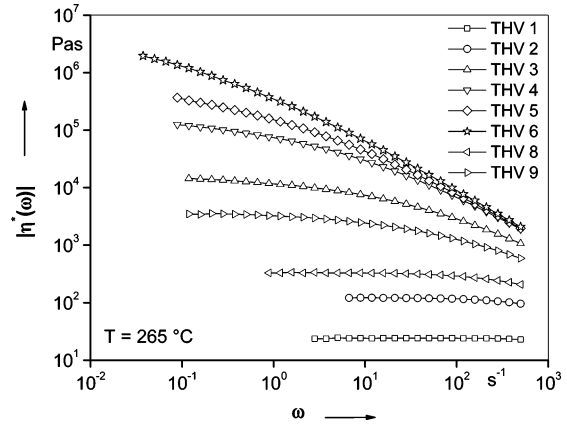

Figure 2. Complex shear viscosity $|\eta^*(\omega)|$ as a function of the angular frequency ω for several linear THV.

comparable contraction factors g_η, but due to the different amounts of the transfer agent employed, different molar masses were obtained.

Auhl et al.[11] could show that the branching topography is similar for all samples under investigation, as proven by the same molar mass dependence of the contraction factor in a reduced molar mass plot.

Thermal Stability. Obviously, viscoelastic properties of polymers can only be determined if their thermal stability under measuring conditions is sufficient. To check the thermal stability during the rheological measurements, time sweeps were conducted for all samples at a constant frequency of 1 s^{-1} in a nitrogen atmosphere of 265 °C (this was the highest temperature applied in this study). A 10% deviation from the initial value of $G'(\omega)$ was defined as the threshold for thermal stability. As illustrated for two linear and two long-chain branched samples in Figure 1, this stability criterion is fulfilled for at least 10^4 s, which was sufficient for most of the experiments.

Oscillatory Shear Flow. The shear flow behavior of the THV samples was characterized by means of oscillatory experiments at a constant temperature of 265 °C. The dynamic shear viscosities $|\eta^*(\omega)|$ of several linear THV samples covering a broad range of molar masses are plotted as a function of the applied frequency in Figure 2. For the linear THV with mass-average molar masses below 500 kg/mol, the Newtonian plateau is reached within the threshold for thermal stability. With increasing molar mass, the applied frequency range more and more covers the shear thinning region of the viscosity curve.

The significant influence of long-chain branching on the linear rheological behavior can be seen in a plot of the phase angle δ versus the absolute value of the complex modulus $|G^*(\omega)|$, often called the Van Gurp−Palmen plot.[12] Because of the narrow molar mass distribution of the linear THV samples, one universal curve is obtained for all linear THV, as can be seen in Figure 3. Any deviation from that curve can be referred to the influence of long-chain branches or a broadening of the molar mass distribution. For the curves of the LCB-THV, a more or less developed bump is observed. As the molar mass distributions only slightly increase from LCB-THV 1 to LCB-THV 4 and can be regarded the same for LCB-THV 3, LCB-THV 5, and LCB-THV 6, some conclusions can be drawn with respect to the branching architecture of the samples. $\delta(|G^*|)$ is shifted downward in comparison to the curve for the linear samples from LCB-THV 1 to LCB-THV 4, as can be seen in Figure 3a. This result gives a hint to a growing influence of branching on the relaxation time spectrum with increasing sample number from 1 to 4, which is in agreement with the rise of the modifier concentration (cf. Table 2).

$\delta(|G^*|)$ does exhibit significant differences, too, for the samples LCB-THV 3, LCB-THV 5, and LCB-THV 6, although they were polymerized with the same modifier content (cf. Figure 3b and Table 2). This result reflects the influence of the molar mass of the branches on the relaxation spectrum, which increases from LCB-THV 5 over LCB-THV 3 to LCB-THV6 (cf. Table 2). The longer the branches are, the stronger is the deviation of $\delta(|G^*|)$ from the curve of the linear products, indicating a rising contribution of the branches to the relaxation spectrum.

Temperature Dependence. Another rheological behavior which depends on branching is the time−temperature superposition. The temperature dependences of the storage and loss moduli were analyzed at temperatures ranging from 140 to 265 °C. These temperature limits are given by the crystallization point on the one side and the thermal stability on the other. The $G'(\omega)$ and $G''(\omega)$ curves of thermorheologically simple fluids can be superimposed by a shift along the frequency axis. The shift factor a is defined then as follows:

$$\log a(T,T_0) = \log \omega(T_0) - \log \omega(T) \tag{3}$$

with T_0 as the reference temperature.

Figure 4 shows the $G'(\omega)$ and $G''(\omega)$ master curves at a reference temperature of $T_0 = 265$ °C for the linear THV 2 and THV 3. The samples show a thermorheologically simple behavior because satisfying superpositions are obtained in both cases.

The shift factors determined from Figure 4 are represented in an Arrhenius plot in Figure 5. All of the values come to lie on a straight line, which means they fulfill the Arrhenius equation:

$$a = a(T_0) \exp\frac{E_a}{kT} \tag{4}$$

E_a follows as 51 kJ/mol and is the same for THV 2 and THV 3 within the accuracy of the measurements. Similar activation energies E_a were found for other linear THV, too. This result indicates that the activation energy is independent of the molar mass, at least within the range given.

Another consequence of the validity of the time−temperature superposition for $G'(\omega)$ and $G''(\omega)$ is that $\delta(|G^*(\omega)|)$ becomes temperature-independent. This is clearly demonstrated for THV 2 in Figure 6. In the case of thermorheologically complex fluids, $G'(\omega)$ as well as $G''(\omega)$ cannot be superimposed, as not all the

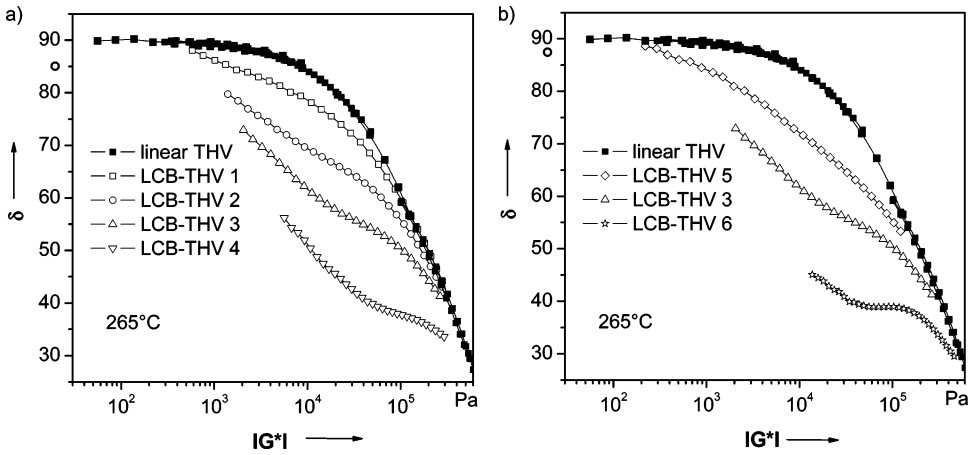

Figure 3. Phase angle as a function of the complex modulus (a) for the LCB-THV 1−4 (increasing amount of branching agent) and (b) for the LCB-THV 3, 5, and 6 (increasing molar mass, constant amount of branching agent) in comparison to linear THV.

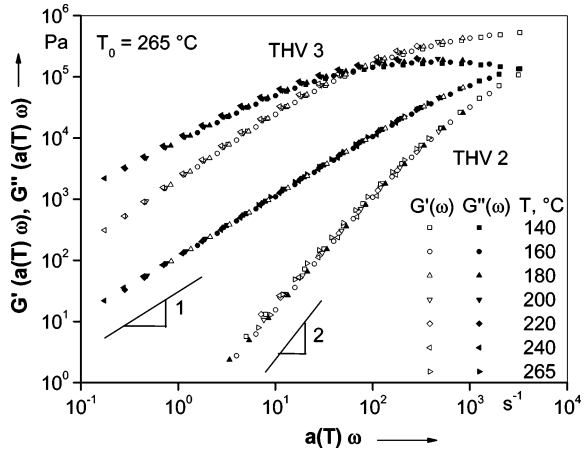

Figure 4. Master curves of $G'(\omega\, a_T)$ and $G''(\omega\, a_T)$ for the linear THV 2 and THV 3.

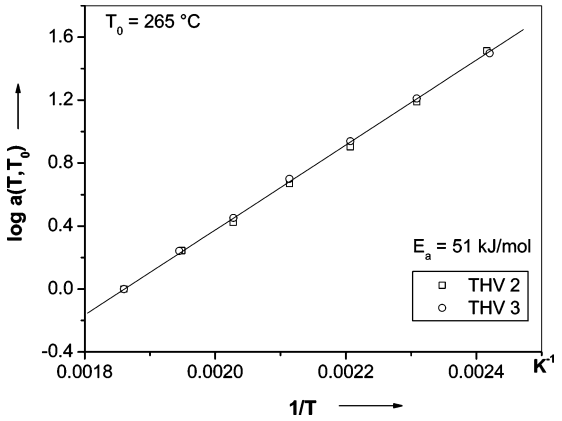

Figure 5. Arrhenius plot of the time−temperature shift factor a_T for the linear THV 2 and THV 3.

relaxation times have the same temperature dependence. Such a behavior is sensitively reflected in $\delta(|G^*(\omega)|)$.

As Figure 6 shows, the three LCB-THV presented are thermorheologically complex. The complexity becomes more pronounced from LCB-THV 1 over LCB-THV 2 to LCB-THV 3, which goes along with an increasing degree of branching. Thermorheological complexity has been reported in the literature for long-chain branched polyolefins.[13−15]

Zero-Shear Rate Viscosity. *Linear THV.* The zero-shear rate viscosity η_0, a key parameter of rheological characterization, could only be reached by oscillatory measurements for the linear

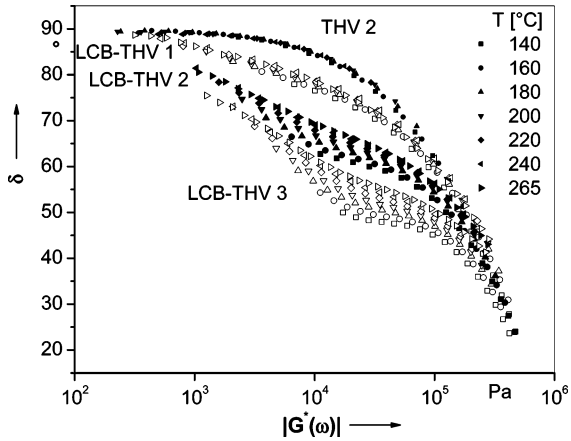

Figure 6. Phase angle δ vs shear modulus $|G^*(\omega)|$ for the linear THV 2 and different LCB-THV.

samples with low molar masses (see Figure 2). If, on the other hand, creep experiments are applied to determine the zero-shear rate viscosity for linear THV samples of high molecular masses, very long measuring times are needed to reach stationary creep flow conditions. This is of concern for samples of mass-average molar masses above 1000 kg/mol, e.g., the linear THV 6, which requires creep times longer than 3×10^4 s to reach a stationary state. Under these conditions, the thermal stability is not given (cf. Figure 1). Consequently, an alternative route to determine the zero-shear rate viscosity had to be taken.

As usually observed for linear polymers of a narrow molar mass distribution, the curves of $G'(\omega)$ and $G''(\omega)$ coincide onto a universal master curve if the frequencies are normalized by the zero-shear rate viscosity. Because all linear THV have an identical polydispersity of well below 2, it should be possible to achieve such a universal master curve for these samples. The applied shift factors used to superimpose the $G'(\omega)$ and $G''(\omega)$ curves of the linear THV samples along the frequency axis are equal to the correspondent zero-shear rate viscosities. $G'(\omega)$ and $G''(\omega)$ were measured at a constant temperature of 265 °C. This reference temperature of 265 °C was chosen as a compromise between the thermal stability of the linear THVs and the aim to reach the terminal zone within the experimental window. The $G'(\omega)$ and $G''(\omega)$ curves of the lower molar mass samples were shifted along the frequency axis using the zero-shear rate viscosities directly attainable from the terminal zone. As can be seen from Figure 7a, the curves of all these products (THV 1, 2, and 8) come to lie on one curve with good accuracy. The curves of the other samples were also shifted horizontally. To

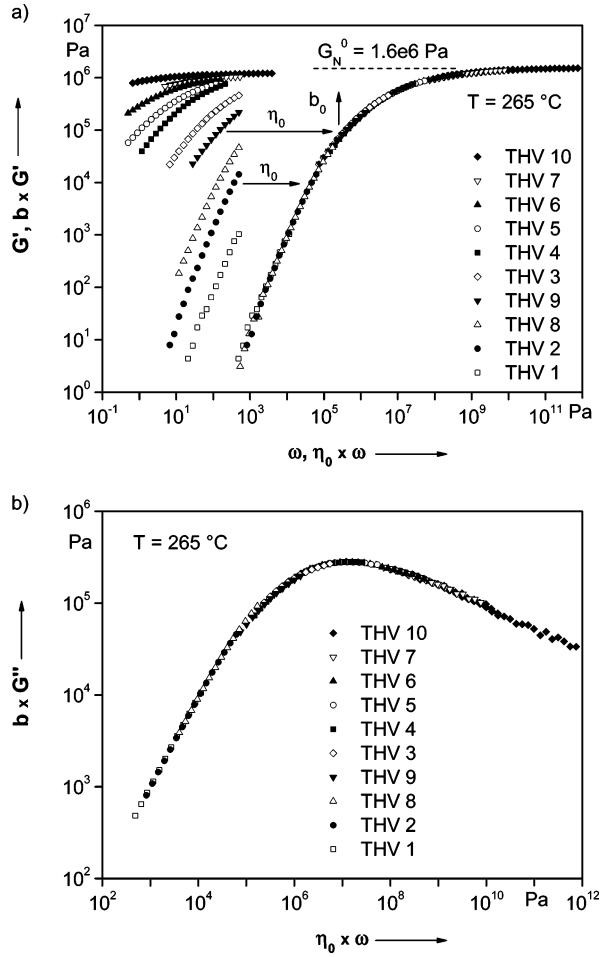

Figure 7. Universal master curves $b\,G'(\eta_0\,\omega)$ (a) and $b\,G''(\eta_0\,\omega)$ (b) of the different linear THV.

achieve a satisfactory superposition of all data sets, additional shifts along the vertical axis were needed, however, for some of the samples of high molecular masses. This shift is related to the fact that the same well-defined sample geometry within the rheometer is difficult to obtain for the high-molar-mass specimens and, therefore, the moduli have to be corrected by a geometrical factor.

The master curves of G' and G'' are presented in Figure 7. The shift factors along the frequency axis which correspond to η_0 are listed in Table 1. Both master curves were obtained by using identical shift factors b and η_0 for each polymer. They cover a very broad frequency range of nearly 10 decades, containing the dynamic-mechanical spectrum from the Newtonian flow region up to the rubbery plateau. The plateau modulus G_N^0 follows as 1.6×10^6 Pa from Figure 7a. The same value for G_N^0 is obtained by an integration of G'' shown in Figure 7b using Ferry's procedure.[16] The value of the plateau modulus lies within the range of literature data reported for other fluoropolymers.[3,17,18] Using the obtained plateau modulus G_N^0 and the melt density ρ_{melt} of the THV polymers at 265 °C of 1.5 g/cm^3, the entanglement molar mass M_e of the THV polymers was determined to be 4100 g/mol according to the equation $M_e = \rho_{melt}\,RT/G_N^0$ in which R is the universal gas constant and T the temperature.

In Figure 8, the η_0 values are presented as a function of M_w in a double-logarithmic plot. The experimental data can be described by a straight line following the equation

$$\eta_0 = k_m \cdot (M_w)^{3.8} \tag{5}$$

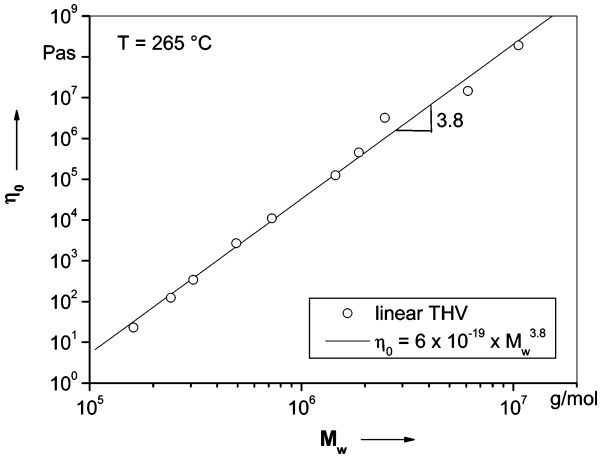

Figure 8. Zero-shear rate viscosity η_0 as a function of M_w for linear THV samples at 265 °C.

with $k_m = 6 \times 10^{-19}$ for η_0 in Pas and M_w in g/mol. The exponent is somewhat higher than those found for other linear polymers like polystyrene and polyethylene, which lie between 3.4 and 3.6.[19−23]

Long-Chain Branched THV. As has been shown for polyethylenes[15,24,25] and polypropylenes,[22,25] some insight into long-chain branching can be obtained by comparing the η_0 values of LCB products with the corresponding data of linear counterparts of the same absolute mass-average molar mass.

To apply these results to THV, the zero-shear rate viscosities of the long-chain branched THV samples were determined from oscillatory shear experiments at 265 °C. For the LCB-THV samples 1 and 5, the terminal zone could be reached within the frequency range applied. For the other samples, the zero-shear rate viscosity was determined using the extrapolation of the measured curve $\eta(\omega)$ according to the Carreau formula.[23] The values of the zero-shear rate viscosities of the long-chain branched THV samples obtained from the dynamic-mechanical measurements are summarized in Table 2.

The η_0 values obtained by this method have to be taken with care as they depend on the kind of material and the set of experimental data available. Significant deviations from the real value can occur. This is particularly the case for materials of a broad relaxation time distribution. Therefore, the zero-shear viscosities of some of the LCB-THV were determined additionally by creep experiments. Because of the fact that long creep times are needed to reach a steady state, a lower temperature of 200 °C was applied in order to stay in the stability window during the experiment. A steady-state value of $t/J(t)$ could be attained in the creep experiments for the four long-chain branched THV samples LCB-THV 1−3 and LCB-THV 5 (cf. Figure 9).

From the coincidence of the $t/J(t)$ curves of LCB-THV 3 measured with the applied stresses of 10 and 20 Pa (cf. Figure 9), it is concluded that the creep experiments performed at $\tau_0 \leq 20$ Pa were conducted in the linear range. A steady state was not reached for the high-molecular LCB-THV 4 and 6, presumably due to insufficient thermal stability. The zero-shear rate viscosities obtained from the creep experiments at 200 °C were shifted to 265 °C by time−temperature superposition using the flow activation energies determined from creep experiments at different temperatures. The η_0 values obtained in this way are given in Table 2, too. The agreement with the data directly obtained from the dynamic-mechanical measurements is very good (cf. LCB-THV 1 and LCB-THV 5) and moderate with the extrapolated values.

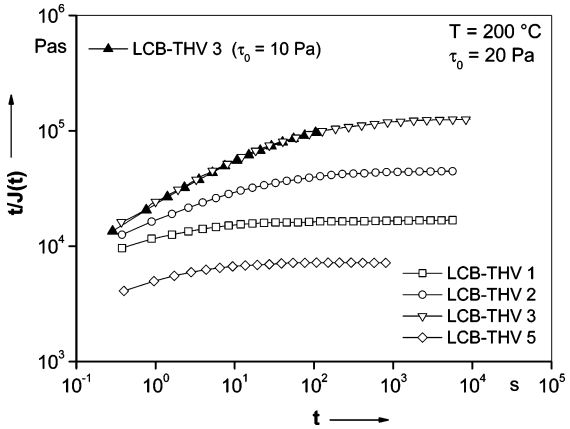

Figure 9. Ratio of $t/J(t)$ of linear and long-chain branched THV samples at 200 °C.

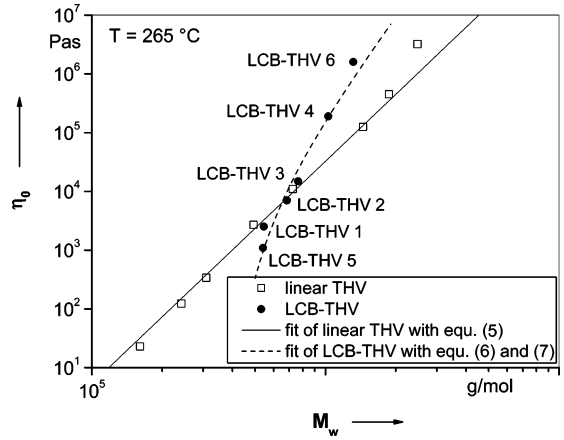

Figure 10. Zero-shear rate viscosity η_0 as a function of M_w for linear and long-chain branched THV samples at 265 °C.

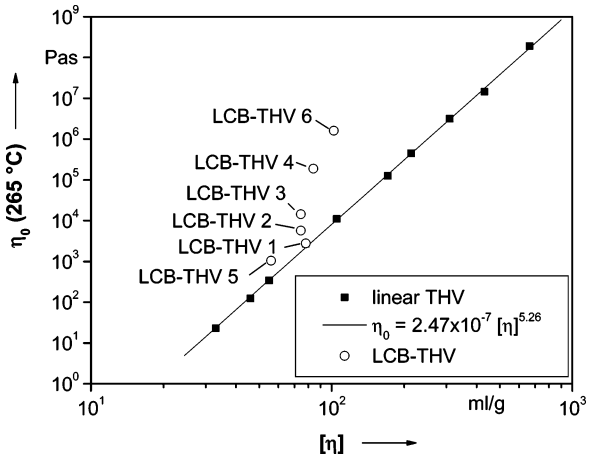

Figure 11. Dependency of the zero-shear rate viscosity η_0 on the intrinsic viscosity $[\eta]$ for linear and long-chain branched THV.

Comparison of $\eta_0(M_w)$ for the Linear and Branched Samples. The zero-shear rate viscosities are plotted in Figure 10 double-logarithmically versus the absolute mass-average molar mass determined by SEC-MALLS. The values of the linear THV are presented by the linear regression line with a slope of 3.8. Some points come to lie above, others below the line, representing the linear products. Such a behavior has been observed for LCB-PE and LCB-PP, too. Typically, polymers with branches of high molar masses, such as metallocene-catalyzed polyethylenes, exhibit an elevated zero-shear rate viscosity compared to a linear reference of the same molar mass.[15,24,25] For highly branched polymers with branches of lower molar masses, η_0 comes to lie below the line for linear samples. Such a behavior is, for instance, found for LDPE.[25,26]

Taking these findings into account, the results on the various LCB-THV samples presented in Figure 10 can be understood. The high-molecular-mass samples LCB-THV 4 and 6 show a distinctly increased zero-shear rate viscosity compared to the η_0-M_w correlation of the linear THV. This indicates that these samples contain long-chain branches of high molar masses. In contrast, a zero-shear rate viscosity below the line for linear THV is found for the LCB-THV 5.

For a more quantitative description of the dependence of the zero-shear rate viscosity on molecular weight for randomly branched polymers like the LCB-THV samples investigated, Janzen and Colby[27] proposed the following relationships:

$$\eta_0 = \begin{cases} AM_w \text{ for } M_b < M_c & \text{(6a)} \\ AM_w\left[1 + \left(\frac{M_w}{M_c}\right)^{2.4}\right] \text{ for } M_c < M_w < M_b & \text{(6b)} \\ AM_b\left[1 + \left(\frac{M_b}{M_c}\right)^{2.4}\right]\left(\frac{M_w}{M_b}\right)^{s/\gamma} \text{ for } M_c < M_b < M_w & \text{(6c)} \end{cases}$$

Here M_c is a critical molar mass for the entanglement of random branches, M_w is the mass average molar mass, and M_b is an average molar mass between a branching point and its adjacent vertices, either chain ends, or other branches. A is a numerical prefactor specific for a chosen polymer system at a given temperature. M_c equals 2.5 times the molar mass of entanglements M_e ($M_c = 2.5\ M_e$), whereas M_e of THV was determined as 4100 g/mol.

Equation 6b describes the usual 3.4-power dependence of η_0 on M_w for linear polymers with $M_w \gg M_c$. [Janzen and Colby[27] could show that, in the case of randomly branched polymers with a nearly constant M_b, those polymers with a lower M_w than M_b followed the relationship in eq 6b, which means that those polymers did not contain long-chain branches.] As for linear THV, a 3.8-power dependence was found; the exponent in eqs 6b and 6c is assumed to be 2.8 instead of 2.4. Applying eq 6b to the results of the linear THV samples, the prefactor A was determined as $A = 9.5 \times 10^{-8}$ Pas/(g/mol).

Equation 6c is assumed to be valid for the long-chain branched THV. The exponent s/γ can be derived from molecular parameters as follows:

$$\frac{s}{\gamma} = \max\left[1, \frac{3}{2} + \frac{9}{8}B \ln\left(\frac{M_b}{90M_{Kuhn}}\right)\right] \quad (7)$$

Here B is another prefactor and M_{Kuhn} is the molar mass of a Kuhn segment. If M_b and M_{Kuhn} are known, the prefactor B can be determined by fitting eqs 6c and 7 to our results of η_0 and M_w of the long-chain branched THV.

The average molar mass between a branching point and its adjacent vertices M_b can be determined from SEC-MALLS using the theory of Zimm and Stockmayer[28] under the assumption, that the branching topography can be described by a Cayley tree with three-functional branching points. As described in a previous paper by Auhl et al.,[11] the LCB-THV investigated fulfill this assumption. In this case, M_b can be determined by dividing the mass-average molar mass of the branched THV by the total number of edges b:[27]

$$M_b = \frac{M_w}{b} \quad (8)$$

Table 3. Parameters for Fitting eqs 6 and 7 to the Results of the Investigated LCB-THV

parameter	value	source
A, (Pas)/(g/mol)	9.5×10^{-8}	fitting eq 6b to the results of the linear THV samples
B	1.85	fitting eqs 6c and 7 to the results of the LCB-THV
M_m, (g/mol)	43.75	molar mass of a C-unit in the THV-backbone
M_e, (g/mol)	4142	
M_c, (g/mol)	10 355	2.5 M_e
M_{Kuhn}, (g/mol)	14.3 M_m	estimated from $L_{Kuhn} = 6\,[\langle s^2\rangle^{1/2}]^2/P_n \times C^{0.5} \times b_0$, with $\langle s^2\rangle^{1/2} = 2.66 \times 10^{-2} \times M^{0.53}$ and assuming the same chain flexibility as polyethylene with $b_0 = 0.154$ nm and $C_\infty^{0.5} = 2.5$

The total number of edges b is related to the weight-average number of branching points n_3 by the following equation:[27]

$$b = 2n_3 + 1 \tag{9}$$

whereas n_3 can be determined from the average molar mass of a polymer subunit λ:[11]

$$n_3 = \frac{M_w}{\lambda} \tag{10}$$

λ was determined from the light-scattering data according to the theory of Zimm and Stockmayer[28] as described by Auhl et al.[11] The values for λ and M_b are given in Table 2.

Using the parameters given in Table 3 and the values for M_b (Table 2), eqs 6c and 7 were fitted to the measured data of $\eta_0(M_w)$ of the branched products. The resulting curve is shown in Figure 10 as a dashed line. For the fit parameter B, a value of $B = 1.85$ was determined. As can be seen from Figure 10, the measured data can very well be described by eq 6c. This indicates that the dependency of the zero-shear rate viscosity on the mass-average molar mass of the long-chain branched THV polymers investigated can be related to the molecular structure and mainly to the average molar mass between a branching point and its adjacent vertices M_b or the average molar mass of a trifunctional monomeric subunit λ, respectively.

A very sensitive method for the detection of LCB can be expected from a relationship between $\eta_0(M_w)$ and $[\eta](M_w)$, as both quantities react on the existence of LCB. For linear THV, the following equation describes the dependency of $[\eta]$ on M_w

$$[\eta] = k_s \cdot (M_w)^a \tag{11}$$

with k_s and a being constants specific for linear THV and the solvent used.

Combining eqs 5 and 11 leads to

$$\eta_0 = k \cdot [\eta]^b \tag{12}$$

with $k = k_m\, k_s^{-3.8/a}$ and $b = 3.8/a$.

As the experimental data in Figure 11 show, this relationship is fulfilled for the linear samples investigated. The values for k and b are given in Figure 11. As expected, significant deviations from eq 12 are found for the long-chain branched THV (Figure 11). Compared with Figure 10, the deviation of the zero-shear rate viscosity from the relationship for the linear references is most pronounced for the sample of high LCB content (LCB-THV 4) and for the sample bearing branches of high molecular mass (LCB-THV 6). Moreover, clear deviations from eq 12 can already be seen if the molecules are only moderately branched. Using $\eta_0(M_w)$, it was not possible to assess the branched character of LCB-THV 2 and 3 (Figure 10). These samples can clearly be discriminated from the linear THV in the plot of Figure 11.

An interesting behavior is found for LCB-THV 5, which was synthesized with the same amount of branching agent as LCB-THV 3 and 6, but has a lower molar mass. As a result, the molar mass of the long-chain branches can be expected to be low, too, thus leading to a reduction of the zero-shear rate viscosity compared to a linear THV of the same molar mass (see Figure 10). Comparing Figure 10 to Figure 11, it becomes obvious that a plot of η_0 vs $[\eta]$ is more sensitive to discriminate between the various LCB-THV than η_0 vs M_w. The disadvantage, however, is that a convincing model describing η_0 as a function of $[\eta]$ is not available.

Conclusions

It has clearly been demonstrated that the new class of long-chain branched THV polymers can very effectively be characterized by using rheological methods in the linear-viscoelastic regime. Dynamic-mechanical measurements represented as the phase angle δ as a function of the magnitude of the complex modulus $|G^*|$ showed significant differences between the samples. Applying this method, it has to be taken into account, however, that it reflects the relaxation spectrum, which is influenced by both the molar mass distribution and the branching architecture. As the polydispersity factor does not change much between the samples, qualitative conclusions with respect to long-chain branches could be drawn. This is particularly the case for the three specimens with a very similar number of branching points but different lengths of the branches, as their polydispersity factors were very similar. The plot $\delta(|G^*|)$ revealed a significant effect of the molar mass, which may contribute to a growing length of the branches.

A behavior not influenced by polydispersity but reflecting the presence of long-chain branches is the time−temperature superposition. Exploiting this principle by measuring the temperature dependence of $\delta(|G^*|)$ pointed to a high sensitivity, as already small amounts of branches were indicated by deviations from the temperature-independent master curve. Conclusions with regard to the architecture of the branches cannot be drawn, however, from these results, as there is no underlying model that relates the molecular structure to time−temperature superposition.

A very sensitive indicator of long-chain branches is the zero-shear rate viscosity η_0 if plotted as a function of the absolute mass average molar mass M_w measured by light scattering. It was possible to quantitatively describe the experimental results using an approach proposed by Janzen and Colby. Two of the parameters were taken from the relationship between η_0 and M_w for the linear samples; others were determined by assuming a Cayley tree with three functional branching points for the molecular architecture.

Assumptions had to be made with respect to the estimation of the so-called Kuhn length. It was calculated from the radius of gyration measured by light scattering.

The good description of $\eta_0(M_w)$ of the long-chain branched THV by the model proposed by Janzen and Colby leads to two

conclusions. First, the assumption of a three-functional reaction mechanism is supported by the rheological measurements. Second, the molecular parameters following from characterizations in the highly diluted state, like the radius of gyration and the average molar mass of a polymer subunit, do not change much if considered in the solid state.

Acknowledgment. We thank the Bayerische Forschungsstiftung for the financial support of this work conducted within the Fluka project (file no. 608/04). We also gratefully acknowledge the support and the valuable comments from Joachim Kaschta and Dietmar Auhl of the Institute of Polymer Materials at the Friedrich-Alexander-University Erlangen-Nürnberg.

References and Notes

(1) Rosenbaum, E. E.; Hatzikiriakos, S. G.; Steward, C. W. *Rheol. Acta* **1998**, *37*, 279−288.
(2) Ayad, D.; Carrot, C.; Guillet, J. *Int. J. Polym. Anal. Charact.* **2001**, *6*, 619−937.
(3) Wu, S. *Macromolecules* **1985**, *18*, 2023−2030.
(4) Tuminello, W. H. In *Encyclopaedia of Fluid Mechanics, Vol. 9, Polymer Flow Engineering*; Gulf: Houston, TX, 1986; pp 209−242.
(5) Micic, P.; Bhattacharya, S. N.; Field, G. *Polym. Eng. Sci.* **1998**, *38*, 1685−1693.
(6) Debbaut, B.; Goublomme, A.; Homerin, O.; Koopmans, R.; Liebman, D.; Meissner, J.; Schroeter, B.; Reckmann, B.; Daponte, T.; Verschaeren, P.; Agassant, J. F.; Vergnes, B.; Venet, C. *Int. Polym. Process.* **1998**, *13*, 262−270.
(7) Münstedt, H.; Steffl, T.; Malmberg, A. *Rheol. Acta* **2005**, *45*, 14−22.
(8) Münstedt, H.; Kurzbeck, S.; Stange, J. *Polym. Eng. Sci.* **2006**, *46*, 1190−1195.
(9) Maccone, P.; Apostolo, M.; Ajroldi, G. *Macromolecules* **2000**, *33*, 1656−1663.
(10) Kaspar, H.; Hintzer K.; Zipplies, T.; Kaulbach, R.; International Patent WO 04/094491A1, 2004.
(11) Auhl, D.; Kaschta, J.; Münstedt, H.; Kaspar, H.; Hintzer, K. *Macromolecules* **2006**, *39*, 2316−2324.
(12) van Gurp, M.; Palmen, J. *Rheol. Bull.* **1998**, *64*, 5−8.
(13) Raju, V. R.; Rachapudy, H.; Greassley, W. W. *J. Polym. Sci.* **1979**, *17*, 1223−1235.
(14) Laun, H. M. *Prog. Collid Polym. Sci.* **1987**, *75*, 111−139.
(15) Malmberg, A.; Liimatta, J.; Lehtinen, A.; Löfgren, B. *Macromolecules* **1999**, *32*, 6687−6696.
(16) Ferry, J. D. *Viscoelastic Properties of Polymers*; John Wiley & Sons: New York, 1980.
(17) Tuminello, W. H., *Polym. Eng. Sci.* **1986**, *26*, 1339−1347.
(18) Wu, S. *Polym. Eng. Sci.* **1988**, *28*, 538−543.
(19) Masuda, T.; Kitagawa, K.; Inoue, T.; Onogi, S. *Macromolecules* **1970**, *3*, 116−125.
(20) Struglinski, M. J.; Graessley, W. W. *Macromolecules* **1985**, *18*, 2630−2643.
(21) Gabriel, C.; Münstedt, H. *Rheol. Acta* **2002**, *41*, 232−244.
(22) Auhl, D.; Stange, J.; Münstedt, H.; Krause, B.; Voigt, D.; Lederer, A.; Lappan, U.; Lunkwitz, K. *Macromolecules* **2004**, *37*, 9465−9472.
(23) Stadler, F.; Piel, C.; Kaschta, J.; Rulhoff, S.; Kaminsky, W.; Münstedt, H. *Rheol. Acta* **2005**, *45*, 755−764.
(24) Wood-Adams, P.; Dealy, J. M.; de Groot, A. W.; Redwine, O. D. *Macromolecules* **2000**, *33*, 7489−7499.
(25) Gabriel, C.; Münstedt, H. *J. Rheol.* **2003**, *47*, 619−630.
(26) Münstedt, H., In *Fliessverhalten von Stoffen und Stoffgemischen*; Kullicke, W., Ed.; Huethig und Wepf Verlag: Basel, 1986; pp 238−279.
(27) Janzen, J.; Colby, R. H. *J. Mol. Struct.* **1999**, *485*−*486*., 569−584.
(28) Zimm, B. H.; Stockmayer, W. H. *J. Chem. Phys.* **1949**, *17*, 1301−1314.

MA0626867